Biomass and Bioenergy 194 (2025) 107626

Contents lists available at ScienceDirect

Biomass and Bioenergy

journal homepage: www.elsevier.com/locate/biombioe

Comparative analysis of aspen plus simulation strategies for woody biomass air gasification processes

Usman Khan Jadoon, Ismael Díaz, Manuel Rodríguez *

Departamento de Ingeniería Química Industrial y del Medioambiente, Escuela Técnica Superior de Ingenieros Industriales, Universidad Politécnica de Madrid, C/ José Gutiérrez Abascal 2, 28006, Madrid, Spain

ARTICLE INFO

Keywords:
Biomass air gasification
Kinetic modeling
Thermodynamic modeling
Renewable energy
Syngas

ABSTRACT

Biomass gasification is gaining attention because of its role in transition to a low-carbon chemical industry, providing a cleaner alternative to fossil fuels in energy and chemical production. However, accurate modeling remains challenging due to the variability in syngas composition across varying biomass types, gasifiers, and operating conditions. This study evaluates the performance of thermodynamic equilibrium modeling (TEM), restricted thermodynamic modeling (RTM), and kinetic modeling (KM) by Aspen Plus to model a fluidized bubbling-bed reactor. The novelty of the research lies in the comparative evaluation of these models in diverse woody biomasses and gasification conditions, addressing a significant gap in the field. Experimental data was curated and used to assess the predictive precision of each approach, focusing on syngas components such as H_2, CO, CO_2, and CH_4. Moreover, sensitivity analysis was performed within the RTM framework to identify optimal approach temperatures for selected. On the basis of these approach temperatures, syngas predictions were carried out, which are referred to as the optimal solution (OS). RTM demonstrated the highest accuracy, with an average RMSE of 0.0793, while TEM showed the lowest accuracy with RMSE of 0.1735. KM and OS had intermediate precision, with RMSE values of 0.1593 and 0.1282, respectively. These results demonstrate that RTM is the most accurate and OS is a reliable alternative when kinetic data are unavailable. This study offers valuable information on the selection of effective modeling strategies for biomass gasification and the development of technologies based on syngas.

1. Introduction

Energy is the essence of life and the foundation of global progress. Ensuring uninterrupted access to energy is crucial to sustained social advancement. Currently, fossil fuels account for approximately 81 % of global energy consumption, with natural gas contributing 23.2 %, oil 30.9 %, and coal 26.8 % [1]. However, this heavy reliance on fossil fuels raises critical concerns about climate change, sustainability, and energy security [2]. To address these issues, the exploration of sustainable and renewable energy sources has become imperative [3]. Unlike finite fossil fuels, which significantly contribute to global greenhouse gas (GHG) emissions, biomass energy presents a potential carbon neutral alternative by utilizing biologically derived compounds to generate diverse energy outputs [4]. Biomass not only has the potential to considerably reduce the carbon footprint of energy production but also enhances energy security by diversifying energy sources and reducing the dependence on fossil fuels.

Biomass energy supports up to 10 Sustainable Development Goals (SDGs), but effective conversion of biomass into useable energy forms requires the adoption of appropriate technologies [5]. Several methods are available for biomass conversion into direct energy (combustion) and fuels, each with distinct advantages. Direct combustion is the most widely used method, which involves the burning of biomass to generate heat for residential heating, industrial processes, and electricity production through steam turbines [6,7]. On the other hand, biomass can also be used in chemical conversion processes such as transesterification, where, for example, it can be used to transform vegetable oils, animal fats and greases into biodiesel [8]. Biological conversion methods, such as fermentation and anaerobic digestion, produce ethanol and biogas, respectively, which serve as fuel for vehicles or renewable natural gas for various applications [9,10]. In the last few years, traditional thermochemical conversion methods such as pyrolysis and gasification have gained interest because of their pivotal role in the production of a variety of fuels. Pyrolysis, performed at temperatures of

* Corresponding author.
E-mail address: manuel.rodriguezh@upm.es (M. Rodríguez).

https://doi.org/10.1016/j.biombioe.2025.107626
Received 15 October 2024; Received in revised form 11 January 2025; Accepted 16 January 2025
Available online 30 January 2025
0961-9534/© 2025 The Authors. Published by Elsevier Ltd. This is an open access article under the CC BY-NC-ND license (http://creativecommons.org/licenses/by-nc-nd/4.0/).

400 °C–500 °C in reduced environment or without O_2, produces charcoal, bio-oil, renewable diesel, CH_4, and H_2 [11]. Hydro-processing of bio-oil obtained from fast pyrolysis at high temperature and pressure with a catalyst can be used to produce renewable diesel, gasoline, and jet fuel [12].

This study focuses on the gasification of woody biomass in bubbling fluidized bed gasifiers (BFBG), which are usually operated at temperatures around 600 °C–950 °C with controlled air injection (sub-stoichiometric O_2), producing syngas rich in CO and H_2. Syngas can be used for different purposes: from electricity generation in gas turbines to the production of chemical compounds such as alcohols (methanol) or dimethyl ether [13,14]. Furthermore, syngas can be further processed using the Fischer–Tropsch process to generate liquid hydrocarbons for transportation (synthetic diesel or kerosene), illustrating the diverse pathways available to harness biomass as an energy and carbon resource [15].

A wide range of gasifier configurations exists, mainly depending on how biomass and the gasifier agent are contacted, fluid and particle movement, and heat transfer management, among other aspects. In the case of solid biomass gasification these reactor configurations include fixed beds, entrained flow gasifiers, fluidized beds, and plasma gasification [16]. Fixed-bed gasifiers, updraft or down draft, are ideal for small-scale applications due to their easy fabrication and operation, producing gas suitable for direct firing [17]. However, they are limited to low moisture raw materials, produce gas with high content of tar, oil, phenol, ammonia, dust content, and require extensive cleanup [18]. Entrained flow gasifiers, on the other hand, have higher costs and complexity, with fuel size restrictions [19]. Solid feedstock must be ground to a small particle size because the residence time of the fuel particles in the hot reaction zone is short (less than 10 s) [20]. Plasma gasification is highly efficient, effectively handling feedstock moisture, tar, and unconverted char. However, it requires extremely high temperatures and consumes 1200–2500 MJ of electricity per ton of biomass or waste, resulting in high operational costs [21]. BFBGs, on the other hand, offer numerous advantages, including easy operation, high heat and mass transfer rates, excellent gas-solid contact, and precise temperature and solid mixing control [22]. They have a good scale-up potential and support continuous in-bed catalytic processing [18]. BFBGs are more tolerant of variations in particle size and higher water content than fixed-bed gasifiers [22]. However, they have higher operational costs compared to fixed-bed gasifiers [23]. Circulating and dual fluidized bed gasifiers face operational challenges more than BFBGs, including higher pressure drops and difficulty with in-bed catalytic processing. They require significant energy input for fans and additional solid separation equipment, leading to increased investment costs and increased process control complexity [24].

The choice of gasifying agents in biomass gasification, including air, steam, O_2-steam, air-steam, O_2-enriched air, CO_2 gasification, O_2-air-steam, or any mixture of these mediums, plays a critical role in determining the quality of syngas [25]. Although the use of O_2 or steam as gasifying agents improves the quality of the syngas in terms of heating value or H_2 content, the high cost and energy consumption of the generation of O_2 or steam have a great impact on process economics (this impact is even higher in small-scale facilities) [26,27]. However, for processes aimed at producing H_2 or Fischer-Tropsch fuels, the use of O_2 or steam can be beneficial despite the increased costs and energy demands. Fluidized air bed gasifiers offer advantages such as cost-effectiveness, energy efficiency, operational simplicity, fuel flexibility, and environmental benefits compared to O_2 or steam-based systems [28]. This makes air a promising gasifying agent for industrial biomass gasification applications.

Numerous research articles on biomass air gasification investigate various operating conditions and types of biomasses, reporting results such as syngas yield, carbon conversion efficiency (CCE), catalyst effects, lower heating value (LHV), and tar production. An experimental study carried out by Katsaros et al. (2020) for the gasification of beech wood and poultry waste found that beech wood produced syngas with LHV of approximately 4.96 MJ/m^3 and a CCE of 91.6 % [29]. In contrast, poultry waste achieved a maximum carbon conversion efficiency of around 86 % and an LHV of approximately 4.2 MJ/m^3, but experienced agglomeration problems at temperatures above 750 °C during gasification. Tian et al. (2023) performed pine sawdust air gasification using raw olivine and Ni/olivine as fluidizing materials and found that the H_2/CO ratio increased from 0.43 with raw olivine to 0.52 with Ni/olivine, and the maximum tar yield decreased from 7.82 mg/Nm^3 to 2.39 mg/Nm^3 [30]. However, LHV decreased from 7.12 MJ/Nm^3 with raw olivine to 6.59 MJ/Nm^3 with Ni/olivine. A similar study by Vincenti et al. (2023) was carried out investigating the gasification of the almond shell with olivine and K-feldspar as fluidizing materials, which determined that olivine tends to produce heavy metal-contaminated syngas, while K-feldspar enables cleaner production of syngas, producing 46 % H_2 compared to 39 % H_2 with olivine [31]. Khezri et al. (2019) conducted an experimental evaluation of the production of Napier grass syngas, achieving a maximum syngas yield of 88.67 %, LHV of 3.59 MJ/Nm^3, and CCE of 90.70 % at 824 °C with an equivalence ratio (ER) of 0.33 and a static bed height of 0.105m, however a decrease in H_2 and CO yield was observed for ER values exceeding 0.33 [32].

Experimenting with different feedstocks and operating conditions to optimize the process is time-consuming and costly. Therefore, computational models and simulations are crucial in predicting the performance of a gasification system. Several tools for modeling biomass gasification have been reported in the literature, including AI-based predictive models, Aspen Plus, ChemCAD, MATLAB, OpenFOAM, and computational fluid dynamics by COMSOL Multiphysics [33–38]. These process modeling tools allow researchers and engineers to model the complex chemical reactions, fluid dynamics, and heat/mass transfer involved in biomass gasification. This helps to predict the gas content of the outlet, optimize operating conditions, and improve the economic efficiency of the gasification process. However, Aspen Plus offers significant advantages for modeling and simulating biomass gasification processes. Its flexibility and versatility allow the configuration and optimization of the entire gasification process under various operating conditions using a wide range of process blocks [39].

To efficiently predict the syngas composition in biomass air gasification, two modeling approaches are commonly employed in the literature: equilibrium and kinetic modeling. Equilibrium modeling can be subdivided into stoichiometric and non-stoichiometric methods. The stoichiometric approach relies on equilibrium constants, whereas the non-stoichiometric method uses Gibbs free energy minimization, which requires minimal setup information for process description and interpretation [40]. Shahlan et al. (2018) presented a simple equilibrium model for optimal gasification conditions of empty fruit bunch biomass that at 850 °C and 1 atm pressure, with higher temperatures increasing H_2 and CO production while reducing CO_2 and CH_4 yields [41]. Hannula et al. (2010) developed a non-stoichiometric model that was validated using experimental data from a scale test rig with various biomasses [42]. A relative error of approximately 14 % was present in the prediction of syngas, and the model appears to be suitable for simulating the gasification of pine sawdust, pine, eucalyptus wood chips, and forest residues, but it is not suitable for pine bark or wheat straw. A study by Mahmut et al. (2019) found that in steam biomass gasification at 770 °C, the experimental H_2 content (vol %, dry basis) in syngas was 53.2 %, with the restrictive model predicting 54.5 % and the equilibrium model 59.8 %, and syngas yields (Nm^3, dry gas/kg-daf-biomass) of 1.72, 1.92, and 2.196, respectively [43]. The restricted chemical equilibrium method, which imposes constraints on the equilibrium reaction temperature, provides better gas composition predictions than the standard chemical equilibrium model, as detailed in the review by Ajorloo et al. (2022) of biomass gasification equilibrium models [44]. In addition to the equilibrium-based modeling approach, hybrid models have been developed that combine equilibrium calculations with empirical

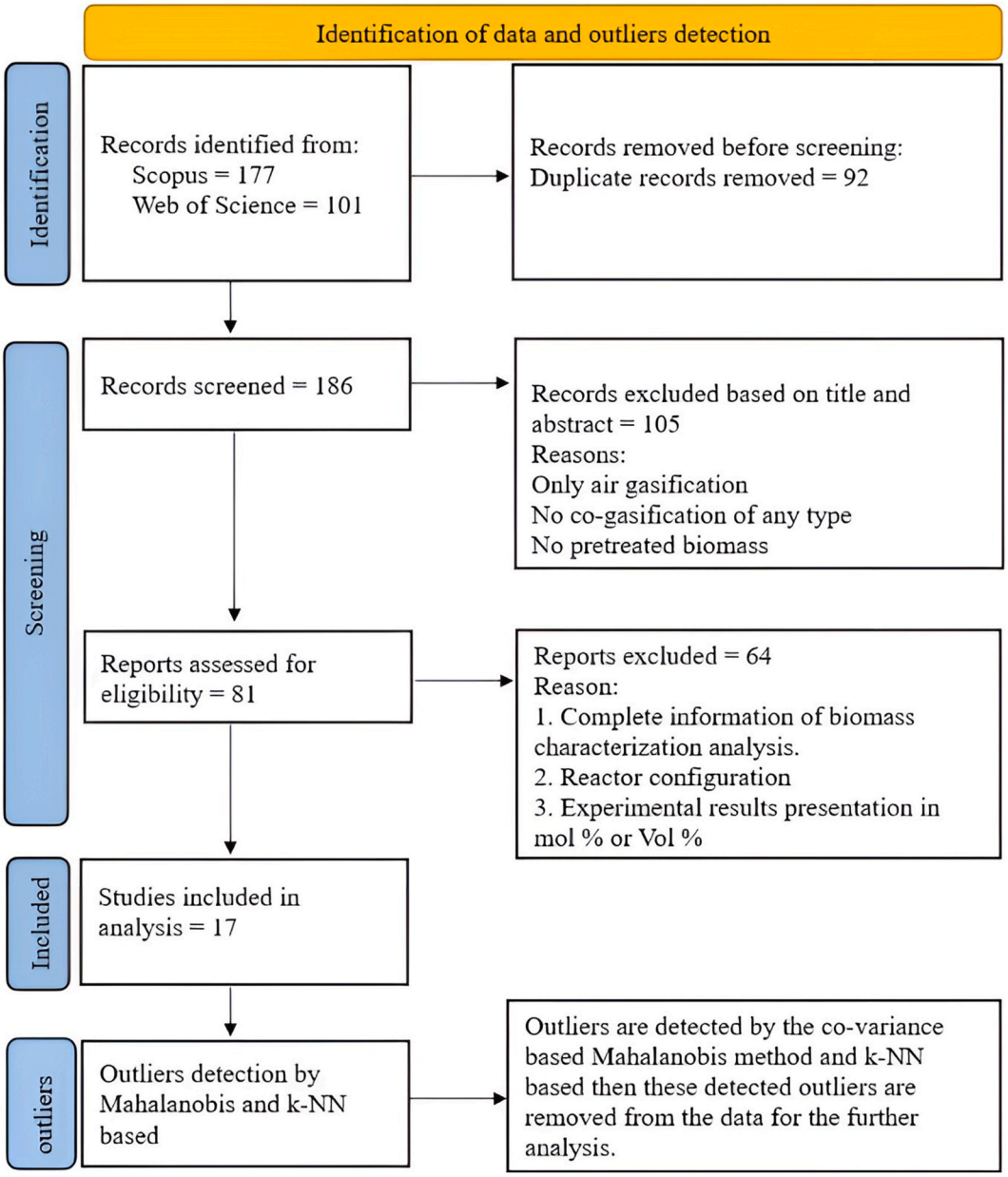

Fig. 1. Experimental data retrieval from literature.

correlations derived from experimental data to improve the precision of predicting the syngas composition in BFBG systems [45].

Although equilibrium models provide a good starting point for simulating biomass gasification in BFBGs, they may not capture the complex kinetic and hydrodynamic phenomena that occur in the reactor [46]. Incorporating additional kinetic models can help to improve the predictive capabilities of the overall simulation approach. The kinetic modeling approach involves the development of a detailed kinetic model that simulates the complex thermochemical reactions that occur during the gasification process. A study by Dhrioua et al. (2002) developed a comprehensive kinetic model for biomass gasification that accurately predicts gaseous species, char and tar yields, and the model was validated against experimental data, showing good agreement [47]. A study by Hernández et al. (2023) on four biomasses with a particular interest in the gasification of sargassum biomass for quality syngas found a lower heating value ranging from 2.6 to 4.8 MJ/Nm^3 for different ER [48]. Similarly, a comprehensive study by Puig-Gamero et al. (2021) included empirical equations for the prediction of pyrolysis products at different temperatures for four different biomasses, revealing that the maximum CCE was 80.78 % at an ER of 0.25 and a bed temperature of 854 °C for pine pellets, while the predicted tar concentrations ranged between 20 and 42 g/Nm^3 for biomasses [49]. To the best of the author's knowledge, there is no existing study that provides a comprehensive comparative assessment of equilibrium, restricted equilibrium, and kinetic modeling approaches. Therefore, this study investigates the efficacy of these modeling approaches in predicting syngas composition using experimental data across varying process variables.

Review of the literature reveals that while equilibrium and kinetic modeling approaches offer valuable insights into biomass gasification processes, there are still inconsistencies in accurately predicting syngas composition. Furthermore, there is a lack of comparative studies that effectively guide researchers during the modeling of biomass gasification processes. Addressing this gap, this study conducts a comparative analysis of modeling approaches focused exclusively on woody biomass air gasification in bubbling fluidized beds. The unique contributions of

Table 1
Experimental data collected from the published works.

ID	Author	Year	Biomass	Experiment	Reference
1	Gomez-Barea et al.	2005	Olive waste (orujillo)	Pilot Scale	[50]
2	Arena et al.	2010	Beechwood	Pilot Scale	[51]
3	Kaewluan et al.	2011	Rubber wood chips	Pilot Scale	[52]
4	Lahijani et al.	2011	Palm empty fruit bunch	Pilot Scale	[53]
5	Kawapinska et al.	2015	Miscanthus giganteus raw	Lab-scale	[54]
6	Serrano et al.	2015	Cynara cardunculus	Lab-scale	[55]
7	Robinson et al.	2016	Wood pellets	Pilot Scale	[56]
8	Nilsson et al.	2017	Olive Tree Pruning	Lab-scale	[57]
9	Pio et al.	2017	Eucalyptus type A, wood pellets, and pine RFB[a]	Pilot Scale	[58]
10	George et al.	2018	Saw dust and coffee husk	Lab-scale	[59]
11	Khezri et al.	2019	Napier grass	Lab-scale	[60]
12	Lan et al.	2019	Pine chips	–	[61]
13	Hai et al.	2019	SRC[b] willow	Pilot Scale	[62]
14	Timsina et al.	2020	Grass pellets and wood pellets	Lab-scale	[63]
15	Wang et al.	2020	Rice straw pellets	Pilot Scale	[64]
16	Bandara et al.	2021	Grass pellets and wood pellets	Lab-scale	[65]
17	Tian et al.	2023	Pine Saw Dust	Lab-scale	[66]

[a] RFB = refused forest biomass.
[b] SRC = short rotation coppice.

this research include:

1. A comparative evaluation of three modeling approaches to identify their strengths and limitations.
2. Sensitivity analysis within the restricted equilibrium framework to refine approach temperatures for key reactions.
3. Development of an optimal solution for predicting syngas composition on the basis of approach temperatures from sensitivity analysis.
4. Validation of modeling approaches with experimental data to determine the most effective strategy for predicting syngas in biomass air gasification.

2. Methodology

2.1. Data preparation

Experimental data on biomass air gasification was carefully collected through comprehensive literature searches using the Scopus and Web of Science databases. It is significant to note that the data set was rigorously curated to include only experimental results derived from air gasification conducted in BFBGs. The selection of published articles was guided by specific criteria; Fig. 1 illustrates the effective strategy used to retrieve relevant data. Specific selection criteria were applied to ensure consistency and reliability: Only studies focusing exclusively on air gasification (excluding co-gasification) and only lignocellulosic biomass is considered. The selected articles were required to provide comprehensive information on biomass characterization analysis, details about the reactor configuration employed, and to show experimental results in either molar percentage or volume percentage. These criteria minimized the impact of varying gasifier types and ensured a standardized dataset for analysis. A total of 151 samples were thoroughly compiled from a selection of 17 publications, which involved experimentation with 22 different biomass types. This experimental data collected from published studies is given in Table 1. The data set comprises 11 input features that represent the key factors that influence the gasification process. These characteristics are categorized and given as: (i) feedstock compositions, which include ash content (Ash), fixed carbon (FC), volatile matter (V), input moisture (Moist), hydrogen content (H), carbon content (C), nitrogen content (N), and oxygen content (O); and (ii) gasification conditions, comprising the equivalence ratio (ER), gasification temperature (T), and input biomass flow rate (Mbio). The output targets of interest are the concentrations of the main components of syngas, namely H_2, CO, CO_2, and CH_4. The curated data set enables the analysis of complex interactions between input features and the prediction of syngas composition during biomass gasification. The statistical description of the input data collected is given in Tables 2 and 3 shows the range and average of the syngas composition values collected from different experiments.

Table 2
Statistical description of input data.

	Name	Range	Mean	Variance
Feedstock Compositions				
Moisture (% w/w, as received)	Moist	0~18.1	7.193	2.739
Ash (% w/w, dry)	Ash	0.28–13.16	4.365	3.459
Fixed carbon (% w/w, dry)	FC	8.17–20.20	15.191	4.091
Volatiles (% w/w, dry)	V	57.77–85.52	73.990	6.470
Carbon (% w/w, dry)	C	39.13–50.90	46.184	3.017
Hydrogen (% w/w, dry)	H	4.7–7.82	6.001	0.595
Nitrogen (% w/w, dry)	N	0~3.19	0.784	0.764
Oxygen (% w/w, dry)	O	34.72–47.71	42.538	3.424
Gasification Conditions				
Equivalent ratio (−)	ER	0.07–0.45	0.233	0.083
Gasification temperature (°C)	T	600~950	767.963	70.649
Biomass flow rate (kg/h)	Mbio	0.4–100	9.203	12.723

Table 3
Syngas composition of the experimental data collected.

Syngas Composition from Experiments				
	Name	Range	Mean	Variance
H_2 concentration (mol/mol, dry, N_2 free)	H_2	0.079–0.412	0.224	0.069
CO concentration (mol/mol, dry, N_2 free) free) free)	CO	0.156–0.494	0.321	0.067
CO_2 concentration (mol/mol, dry, N_2 free)	CO_2	0.11–0.633	0.357	0.093
CH_4 concentration (mol/mol, dry, N_2 free)	CH_4	0~0.239	0.093	0.036

The ER (also known as the stoichiometric ratio or air-fuel ratio) in the context of gasification processes is defined as the ratio of the actual fuel-to-air ratio to the stoichiometric fuel-to-air ratio required for complete combustion or gasification as given in Equation (1). For combustion processes involving hydrocarbon fuels (such as biomass), the stoichiometric fuel-to-air ratio can be calculated on the basis of the reaction equation and the amount of air required for complete combustion.

$$ER = \frac{\left(O_{2flow\ rate}/biomass_{flow\ rate}\right)_{actual}}{\left(O_{2flow\ rate}/biomass_{flow\ rate}\right)_{stoichiometric}} \quad (1)$$

2.2. Data validation and feature correlation

The data analysis process began with outlier detection employing two robust methodologies: Mahalanobis distance-based outlier detection and k-Nearest Neighbor (k-NN) outlier detection. These techniques were applied to the carefully curated datasets described in section 2.1. The Mahalanobis distance-based outlier detection method statistically identifies outliers by calculating the distance of each data point from the data set centroid, considering the covariance structure of the features. This method is mathematically represented as in Equation (2).

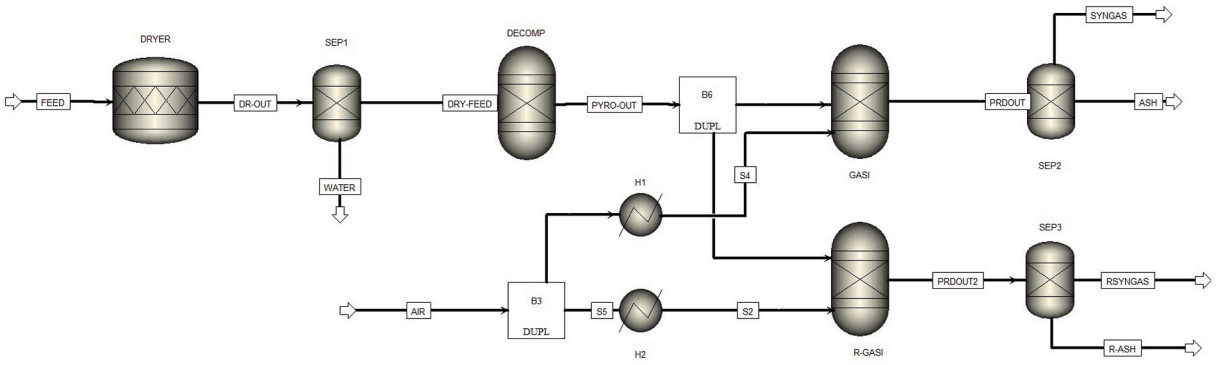

Fig. 2. Aspen Plus flow diagram of TEM and RTM.

$$D_M(x) = \sqrt{(x-\mu)^T \sum^{-1} (x-\mu)} \tag{2}$$

$D_M(x)$ = *is the Mahalanobis distance of data point* x,
x = *data point*,
μ = mean vector of the data set,
Σ = Covariance matrix of the data set.

After the Mahalanobis distances were calculated, the interquartile range (IQR)-based approach was used to identify outliers. The steps included calculating the first (Q1) and third quartiles (Q3) of the Mahalanobis distances, determining the IQR (IQR = Q3−Q1), and setting a threshold for outlier detection. Data points outside the range [Q1−k × IQR,Q3+k × IQR], with $k = 1.5$, were flagged as outliers.

The k-NN outlier detection method identifies outliers based on their distance from neighboring data points. To determine whether a data point *xi* is an outlier using the k-NN approach, follow these steps:

1. Calculate the distance to nearest neighbors: For each data point x_i in the dataset, calculate its distance from its nearest neighbor k. Let $d_i(k)$ denote the distance to the *k*-th nearest neighbor of x_i. In the k-NN method, outlier detection is based on the Minkowski distance with varying p values to assess its impact on outlier identification [67]. The Minkowski distance, defined by Equation (3), is used to calculate the distances between data points x_i and their *k*-th nearest neighbors for different p-values (e.g., p = 2, 3, …), allowing us to assess the impact on outlier identification and ensure a robust analysis of the data set.

$$d_i(k) = \left(\sum_{j=1}^{n} |x_{ij} - x_{kj}|^p \right)^{1/p} \tag{3}$$

2. Define the Outlier Score: The outlier score O_i for each data point x_i is defined based on its distance from the *kth* nearest neighbor and can be defined as given in Equation (4).

$$O_i = \frac{1}{k} \sum_{i=1}^{k} d_i(k) \tag{4}$$

3. Epsilon (ε) incorporation is very crucial in k-NN to set the threshold for the values of k. As ε in density-based spatial clustering of noise applications, the maximum distance between two points must be considered as neighbors.

$$O_i^{\varepsilon} = \frac{1}{k} \sum_{i=1}^{k} \max\left(d_i(k), \varepsilon\right) \tag{5}$$

Where O_i^{ε} is the epsilon based adjusted outlier score.

4. Identify Outliers: The final outlier score for a data point x_i using the k-NN method with ε is expressed as in equation (6).

$$O_i^{\text{final}} = \max\left(O_i^{\varepsilon}, \varepsilon\right) \tag{6}$$

Data points with O_i^{final} values above a certain threshold are flagged as outliers. The k distance plot helps identify a threshold value for the ε, beyond which points are flagged as outliers. Typically, the elbow point in the plot indicates a natural threshold value of the ε at certain value of k (i.e., k = 1,2,3, …). To enhance the robustness of outlier detection, the Minkowski parameter was also varied (e.g., p = 2,3, …) and generated k-distance plots for different values of p. By analyzing these graphs, suitable ε values were analyzed that effectively distinguish between outliers and inliers. In outlier detection, the data set was normalized to ensure that all features were on a comparable scale, thus preventing any feature from disproportionately influencing the outlier detection process.

Additionally, to gain insight into the relationships between input characteristics and their impact on output targets, a Pearson correlation matrix was developed. This matrix quantifies the linear correlation between each pair of input features, providing valuable information on the interdependencies within the data set. This analysis helps to understand the potential influence of individual input features on output targets, facilitating the identification of key factors driving syngas composition in biomass air gasification processes.

2.3. Modeling approaches

Aspen Plus V.14 was used to simulate the biomass gasification process. Both equilibrium-based and kinetic-based models followed a similar initial setup: biomass and char were defined as nonconventional components, with their proximate and elemental analyses specified using the ULTANAL and PROXANAL models. The enthalpy and density data were derived using the HCOALGEN and DCOALIGT models, respectively. HCOALGEN incorporates correlations to calculate heat capacity, heat of combustion, and heat of formation, based on biomass combustion and product formation data. The DCOALIGT model is based on the Institute of Gas Technology (IGT) correlation and is based on the ultimate analysis of the biomass. Ash was also treated as a non-conventional component with a 100 % composition for final and proximate analyzes. The Peng-Robinson thermodynamic package with the Boston-Mathias function was selected for its suitability in high temperature gasification processes [68].

2.3.1. Equilibrium model

Equilibrium-based Aspen Plus modeling is subdivided into two approaches, namely the thermodynamic equilibrium model (TEM) and restricted thermodynamic equilibrium model (RTM). TEM predicts gasification products by minimizing Gibbs free energy, independent of chemical kinetics or stoichiometric constraints. It is computationally efficient and requires minimal inputs, such as biomass elemental

Table 4
Reactions used in a restricted thermodynamic equilibrium model.

R1	$C + 0.5O_2 \rightleftharpoons CO$	(6)
R2	$CO + H_2O \rightleftharpoons CO_2 + H_2$	(7)
R3	$C + 2H_2 \rightleftharpoons CH_4$	(8)
R4	$C + H_2O \rightleftharpoons CO + H_2$	(9)

composition and gasification temperature. This modeling approach has limitations, such as difficulties in accounting for char and tar formation and excluding gasifier geometry and kinetics. It also tends to overpredict H_2 and CO while underpredicting CO_2 and CH_4 [69–71].

RTM improves TEM by restricting reaction equilibria to temperatures above or below the actual reactor temperature, accounting for stoichiometric constraints. This approach is designed to provide a more realistic representation of the gasification process, since the reactions in the reactor may not necessarily reach the true thermodynamic equilibrium. By incorporating temperature-based constraints, it improves the accuracy of syngas composition predictions and other performance metrics. This improved precision is particularly important for optimizing operating conditions and improving the overall efficiency of predicting the syngas composition of biomass air gasification.

In this study, the Aspen Plus-based model of Gu et al. (2019) has been adopted to model the gasification of selected experimental data for TEM and RTM [72]. Fig. 2 illustrates the process flowsheet, comprising three linked processes: pre-drying, decomposition, and gasification. The feed stream is defined using non-conventional components based on the ultimate and proximate analysis of the feedstock.

1. Pre-drying: Wet biomass is pre-dried at 120 °C in an RSTOIC reactor (model ID: DRYER) to reduce moisture content for stable gasification. Moisture is evaporated and separated using a separator (model ID: SEP1).
2. Decomposition: The dried biomass is decomposed in an RYIELD reactor (model ID: DECOM) into its elemental components (H, C, O, N, S, and ash) based on the ultimate and proximate analyses.
3. Gasification: The elemental components are fed into an RGIBBS reactor, where air serves as the gasifying agent to convert the constituents into a gas and solid mixture. The GASI gasifier (model ID: GASI) models TEM by minimizing Gibbs free energy, while the R-GASI reactor (model ID: R-GASI) represents RTM using restricted equilibrium. Heaters H1 and H2 raise the air temperature for the respective reactors, and duplicates B3 and B6 (model ID: DUPL) replicate the output streams of air and DECOMP, respectively. Gas and solids are separated using separators (model IDs: SEP2 and SEP3).

The model assumptions included:

1. Ash is considered inert.
2. Steady-state operation.
3. NH_3 and H_2S were not considered.
4. Tar formation is not considered.
5. Negligible heat loss and pressure drop considered in the model.
6. This approach was 1D.

The comparative analysis for model validation (comparison with experimental data) for both TEM and RTM is given in Supplementary Table S1. Few studies have already been published that have analyzed the comparative study of RTM and TEM. Acar et al. (2019) investigated steam-based gasification modeling of BFBG, employing four reaction sets without specifying the restricted temperatures of the selected reactions [43]. Abdelrahim et al. (2020) validated a restricted chemical equilibrium model using experimental data, finding that RTM was achieved by setting approach temperatures for the four reactions to −286.52 °C, −325.80 °C, 282.81 °C, and 71.08 °C [73]. However, in our study, sensitivity analysis was performed for each sample (151 data samples in total), modifying the temperature approaches of each reaction, to find out temperature ranges for the RTM. The chemical reactions given in Table 4 are considered for the RTM of the gasification process. The temperature ranges in the sensitivity analysis for the selected reactions are as follows: R2 is 0 °C–1000 °C and for R3 and R4 is −1 °C to −500 °C. The change in restricted temperature for R1 does not have a significant effect on the syngas composition; therefore, only the temperature ranges for the reactions R2, R3, and R4 were established after a couple of iterations in the RTM sensitivity analysis.

After a sensitivity analysis using the restricted approach, temperatures approaches were determined in the RTM strategy for the specified reactions along with the syngas composition, comparing these results with experimental data. Each sensitivity analysis generated 29,792 instances, from which that instance was selected that had the lowest absolute difference from the experimental values. This iterative process was repeated for each sample (151), resulting in a collection of different approach temperatures and corresponding syngas compositions for the RTM. Subsequently, the minimum absolute difference across all sensitivity analysis was determined to derive a definitive set of optimal approach temperature values for reactions R2, R3, and R4 based on equation (5). In equation (5) the i = i-th iteration in the sensitivity analysis, exp denotes the experimental value and pred denotes the predicted constituent gas in syngas. Using this finalized set of approach temperatures, the syngas composition was calculated for each sample data, yielding a unique set of syngas composition values based on different ERs, biomass flow rates, gasifier temperatures, and feedstock chemical composition. These new values represent the OS for comparison along with the values from the TEM, RTM, and kinetic models.

$$(\text{Minimum error})_i = |H_2^{exp}\text{-}H_2^{pred}|_i + |CO^{exp}\text{-}CO^{pred}|_i + |CO_2^{exp}\text{-}CO_2^{pred}|_i + |CH_4^{exp}\text{-}CH_4^{pred}|_i \quad (5)$$

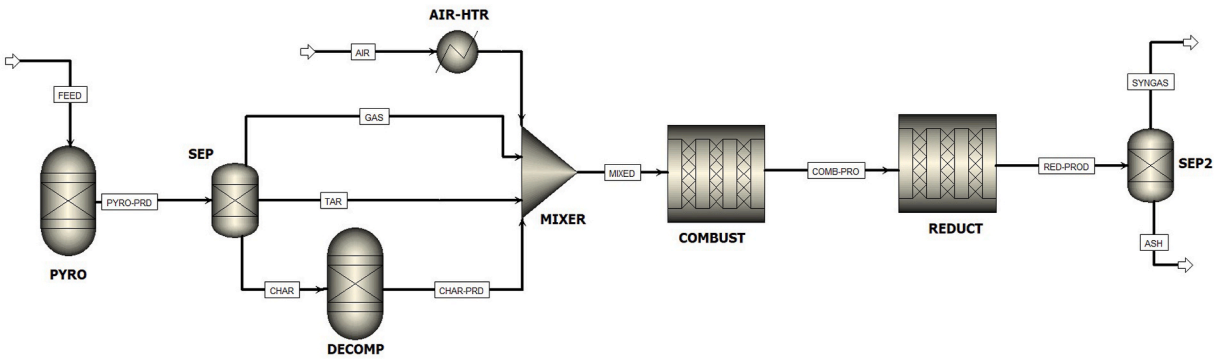

Fig. 3. Aspen Plus flow diagram of kinetic model.

Table 5
Chemical reactions and rate expression used in the kinetic gasification model.

Process	Reaction	Rate Expression	Ref.
Combustion	$aC(s) + O_2 \rightarrow 2(a-1)CO + (2-a)CO_2$	$r_1 = k_1 T e^{(-E/RT)} \frac{6}{D_p}[O_2]$ $a = \frac{1+2f}{1+f}$ with $f = 4.72.10^{-3} e^{(37,787/RT)}$	[75]
	$CO + O_2 \rightarrow CO_2$	$r_2 = k_2.e^{-E/RT}[CO][O_2]^{0.25}[H_2O]^{0.5}$	[76]
	$CH_4 + 0.5O_2 \rightarrow CO + 2H_2$	$r_3 = k_3.e^{-E/RT}[CH_4]^{0.7}[O_2]^{0.8}$	[75]
	$H_2 + 0.5O_2 \rightarrow H_2O$	$r_4 = k_4.e^{-E/RT}[H_2][O_2]$	[76]
	$C_6H_6O + 4O_2 \rightarrow 6CO + 3H_2O$	$r_5 = k_5.e^{-E/RT}[C_6H_6O]^{0.5}[O_2]$	[77]
	$C_6H_6 + 4.5O_2 \rightarrow 6CO + 3H_2O$	$r_6 = k_6.e^{-E/RT}[C_6H_6]^{0.5}[O_2]$	[78]
Reduction	$C + H_2O \rightleftharpoons CO + H_2$	$r_7 = k_7.e^{-E/RT}[C][H_2O]$	[79]
	$C + H_2O \rightleftharpoons CO_2 + H_2$	$r_8 = k_8{}^*e^{-E/RT}[C][H_2O] - \frac{[CO_2][H_2]}{k_{eq}}$ $k_{eq} = 0.0222.e^{34,730/RT}$	[80]
	$CH_4 + H_2O \rightleftharpoons CO + 3H_2$	$r_9 = k_9.e^{-E/RT}[CH_4][H_2O]$	[79]
	$C + CO_2 \rightleftharpoons 2CO$	$r_{10} = k_{10}.e^{-E/RT}[C]$	[79]
	$C_6H_6O \rightarrow CO + 0.4C_{10}H_8 + 0.15C_6H_6 + 0.1CH_4 + 0.75H_2$	$r_{11} = k_{11}.e^{-E/RT}[C_6H_6O]$	[81]
	$C_6H_6O + 3H_2O \rightarrow 4CO + 0.5C_2H_4 + CH_4 + 3H_2$	$r_{12} = k_{12}.e^{-E/RT}[C_6H_6O]$	[81]
	$C_{10}H_8 \rightarrow 6.5C + 0.5C_6H_6 + 0.5CH_4 + 1.5H_2$	$r_{13} = k_{13}.e^{-E/RT}[C_{10}H_8]^{1.6}[H_2]^{-0.5}$	[79]

Table 6
Kinetic parameters of the reactions considered in the kinetic gasification model [49].

Process	Reactions	k	E (J/mol)
Combustion	1	$3.70{\cdot}10^{10}$	$1.50{\cdot}10^{5}$
	2	$1.78{\cdot}10^{10}$	$1.80{\cdot}10^{5}$
	3	$1.58{\cdot}10^{12}$	$2.02{\cdot}10^{5}$
	4	$1.08{\cdot}10^{7}$	$1.25{\cdot}10^{5}$
	5	$6.55{\cdot}10^{2}$	$8.02{\cdot}10^{4}$
	6	$2.40{\cdot}10^{11}$	$1.26{\cdot}10^{5}$
Reduction	7	$8.00{\cdot}10^{-3}$	$4.99{\cdot}10^{4}$
	8	$2.78{\cdot}10^{2}$	$1.26{\cdot}10^{4}$
	9	$3.00{\cdot}10^{13}$	$1.25{\cdot}10^{5}$
	10	$1.05{\cdot}10^{13}$	$1.35{\cdot}10^{5}$
	11	$1.00{\cdot}10^{7}$	$1.00{\cdot}10^{5}$
	12	$1.00{\cdot}10^{7}$	$1.00{\cdot}10^{5}$
	13	$1.00{\cdot}10^{14}$	$3.50{\cdot}10^{5}$

2.3.2. Kinetic model

Kinetic modeling of biomass air gasification in a BFBG is a complex process that involves simulating the intricate thermochemical reactions that occur between biomass feedstock and air. For the kinetic modeling, the Puig-Gamero et al. (2021) model was adopted to model all the experimental data for prediction of syngas [49]. In Fig. 3 shows the process flow diagram of the kinetic gasification model, the inlet process stream, FEED, carries feedstock at a specified flow rate. In the pyrolysis zone, the RYIELD reactor (model ID: PYRO) converts non-conventional biomass into pyrolysis products based on empirical equations from Neves et al. (2011) [74]. These products (PYRO-PRD) are separated into gas, tar, and char using a SEP block. Char is decomposed in the RYIELD reactor (model ID: DECOMP) into C, H, O, S, N, and ash. The pyrolysis products are then mixed with air, preheated by a heater (model ID: AIR-HTR), before undergoing combustion reactions in a PFR block (model ID: COMBUST). The combustion products are reduced in another PFR block (model ID: REDUCT), and the final syngas is separated from the rest using the SEP2 column. The comparative analysis for model validation, presented in Supplementary Fig. S1, is based on the gasification of olive wastes conducted by Gomez-Barea et al. (2005), where the reactor temperature ranged from 740 °C to 820 °C and the ER varied from 0.20 to 0.31 [50]. Kinetic models use rate equations to quantify the rates of various chemical reactions that occur during gasification. These rate equations are typically based on experimental data and can be influenced by factors such as temperature, pressure, residence time, and reactor configuration. The kinetic data used in the combustion and reduction process of this model is given in Table 5 whereas the kinetic parameters are given in Table 6.

The main assumptions considered in the kinetic model are considered below.

1. Ash is considered inert.
2. Steady-state process
3. No heat loss or pressure drop is considered.
4. NH_3 and H_2S are not considered.
5. Although this model considers tar (C_6H_6O, C_6H_6, and $C_{10}H_8$), tar production is not included in the results as the current study focuses on comparative prediction of composition of syngas.
6. Arrhenius kinetics is considered for all rate expressions.

3. Results and discussion

3.1. Data analysis

A total of 151 experimental instances from published articles were used to model biomass air gasification, employing three modeling approaches: TEM, RTM, and KM models. Furthermore, syngas concentrations were determined on the basis of optimal approach temperatures such as OS, resulting in four distinct sets of modeled data for comparison with experimental values. To ensure data integrity and reliability, exploratory data analysis was initially carried out. Outliers were first detected using a combination of covariance-based Mahalanobis distance and k-NN analysis. Through this approach, nine distinct outliers were identified and subsequently removed from the dataset, ensuring the robustness of the subsequent analysis of the input data. Six outliers are

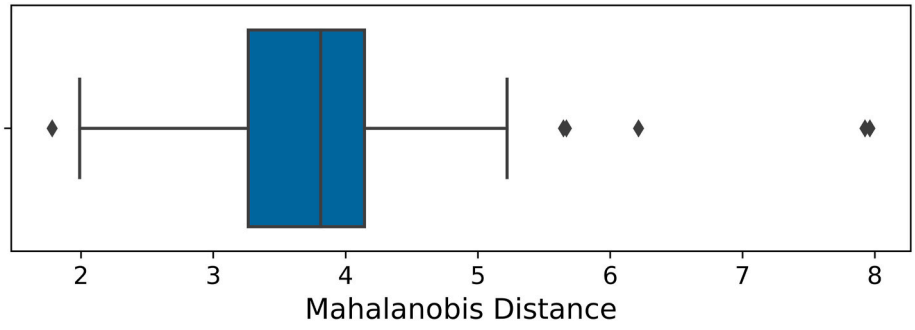

Fig. 4. Outliers based on the Mahalanobis distance by IQR.

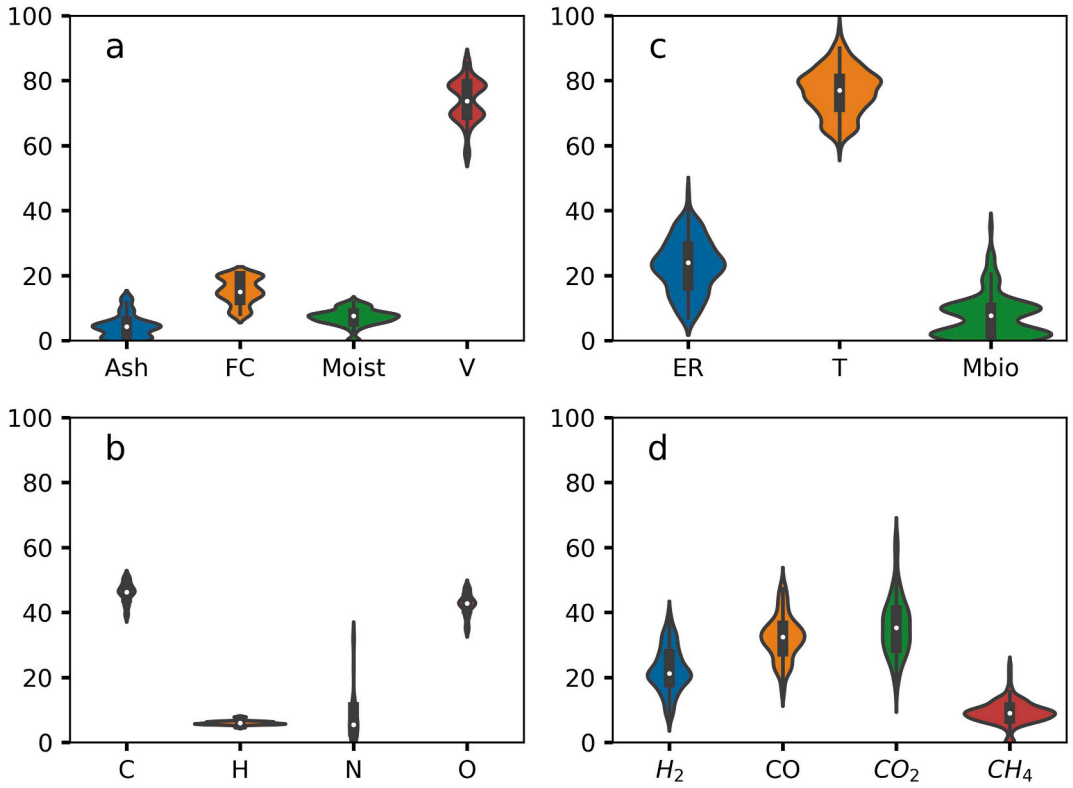

Fig. 5. Statistical representation of the input data (a) proximate analysis (b) ultimate analysis (c) input process variables (d) syngas concentration.

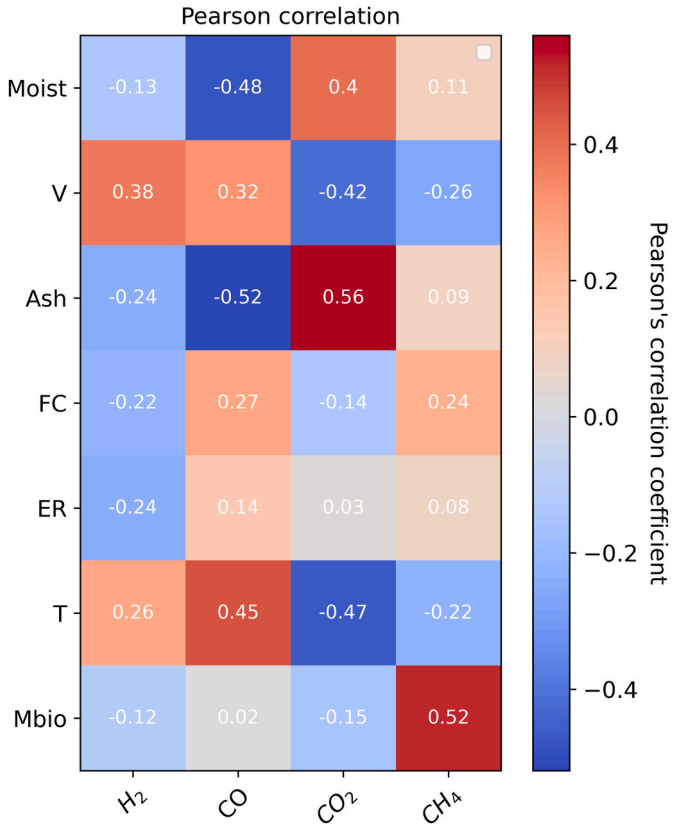

Fig. 6. Pearson's correlation matrix.

detected by the Mahalanobis method, as shown in the box plot in Fig. 4, and five outliers are detected by the k-NN based method, two outliers are similar in both methods. Detailed information on the input data for the various modeling frameworks used in this study can be found in the supplementary data in the Excel file, where outliers are marked in red rows.

To better visualize the relationship between the value of k in the k-NN analysis for the threshold value of ε selection and the resulting distances, detailed graphs were generated and presented in Supplementary Fig. S2. These graphs revealed a consistent pattern across different k values while keeping ε constant. Based on this analysis, k = 2 was selected as the most suitable parameter. Similarly, when examining the Minkowski distance for varying p values against ε, graphs compiled in Supplementary Fig. S3 identified p = 2 as the optimal choice. This analysis resulted in the identification of 23 distinct clusters and five outliers.

The refined dataset, now free of outliers, was subsequently used for further analysis and discussion. The distribution of eleven input characteristics and four experimental outputs was visually represented using the violin plots that contain the IQR plots in Fig. 5, where the wider violins indicate a higher density. To standardize all input variables within the interval (0, 100), the values of N, ER, and T were scaled, respectively. The essential statistical characteristics, including range values, mean values, and standard deviation, are already summarized in Tables 2 and 3.

The Pearson correlation-based matrix, depicted in Fig. 6, outlines the relationships between the input variables and the experimental results. In particular, an apparent pattern emerges with respect to water content (Moist), exhibiting a positive correlation with CO_2 while demonstrating a negative correlation with CO. This phenomenon is probably attributed to its potential influence on the equilibrium of the water-gas shift reaction (WGS), which favors the production of CO_2 and H_2 by shifting the reaction to the right. Consequently, this change results in a decrease in CO content and a simultaneous increase in CO_2 content within syngas generated during biomass gasification processes [82]. Similarly,

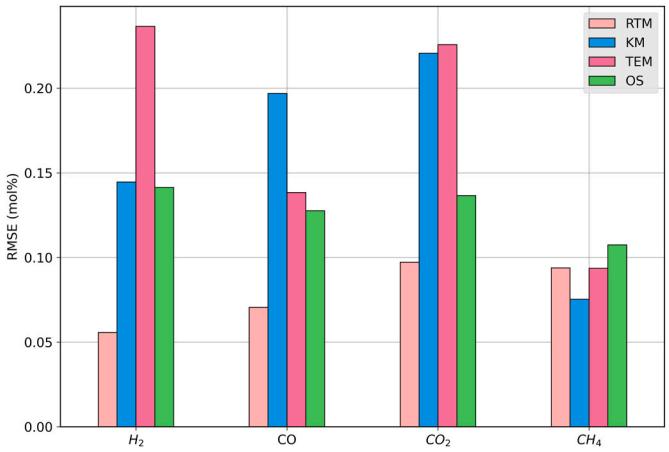

Fig. 7. Root mean square error of syngas prediction model compared to experimental values.

Lampropoulos et al. (2022) investigated the effect of moisture content on syngas composition [83]. According to the study, it has been found that increasing feedstock moisture content also increases the CO_2 content while there is a decrease in the CO concentration. However, the literature does not explicitly address the impact of higher volatile contents in biomass on H_2 production in syngas composition. However, according to Gao et al. (2023), a higher content of volatile matter in biomass can lead to increased production of CO, H_2 and CH_4 in syngas during the gasification pyrolysis stage [84]. Furthermore, a relatively strong positive association between V, H, and C indicates the compositional similarity of the main elements present in V. The increase in reactor temperature in biomass air gasification processes has shown a positive correlation for the generation of H_2 within the syngas. This effect can be due to favorable conditions for the endothermic WGS reaction at higher temperatures [85]. The WGS reaction involves the conversion of CO and H_2O into CO_2 and H_2. Therefore, as the reactor temperature increases, the equilibrium of the WGS reaction changes due to the formation of CO_2 and H_2, thus increasing the H_2 content in the resulting syngas [86].

3.2. Comparative analysis of model predictions

Aspen Plus models that employ TEM, RTM and KM approaches were developed to simulate the gasification of biomass air gasification. For RTM, a detailed sensitivity analysis was performed to determine the optimal approach temperatures for reactions R2, R3, and R4 (Table 4), generating 29,792 cases for the temperature sets and the corresponding syngas concentrations. By minimizing the error between experimental and predicted syngas compositions, the optimal approach temperatures were determined to be 0 °C for R2 and -217.233 °C for both R3 and R4. Using these estimated temperatures, a new set of syngas composition values, called OS values, was generated. These OS values were compared directly with experimental syngas results, allowing a comprehensive evaluation of predictive accuracy along with the RTM, TEM, and KM models.

The results of this study reveal significant differences among the modeling strategies used in the air gasification of woody biomass. The average RMSE corresponding to the different modeling strategies is shown as bar graphs in Fig. 7 (the values are given in the supplementary data in Table S2). In particular, the RTM exhibited the most favorable

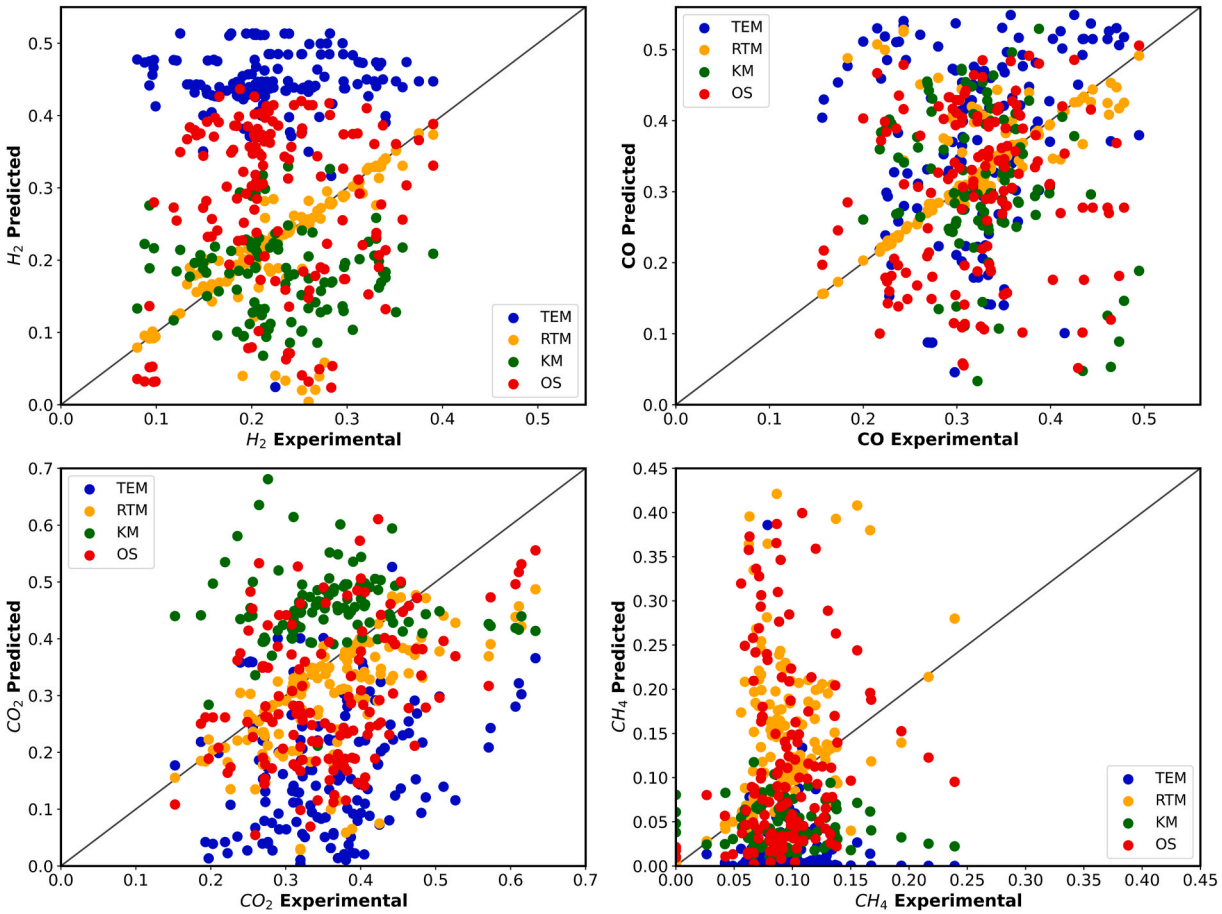

Fig. 8. Scatter plot between experimental and predicted values.

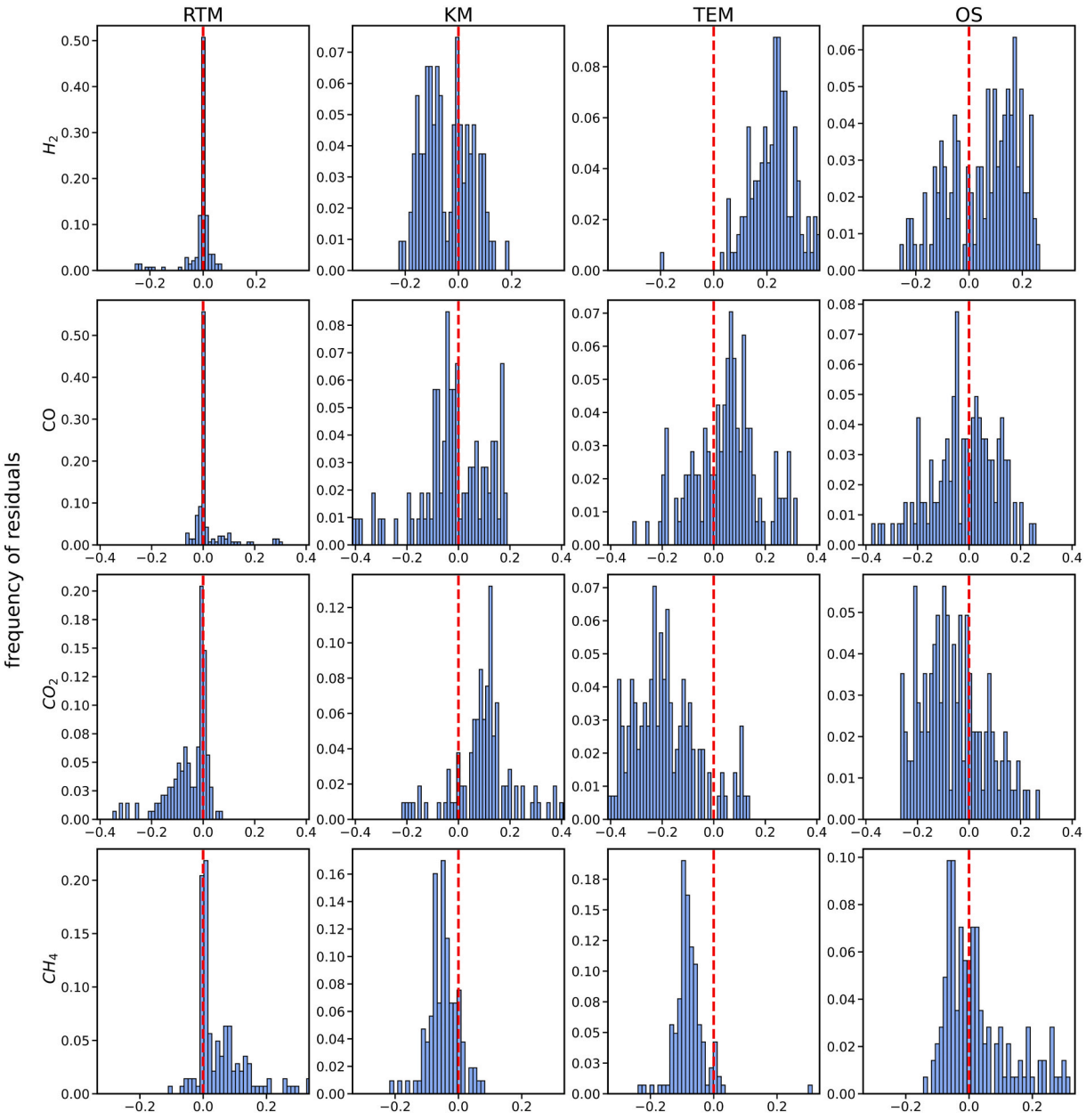

Fig. 9. Residuals of the syngas composition against the experimental values.

performance, having the lowest RMSE values among the three strategies, indicating its superior precision in predicting the composition of syngas compared to the other models. This is because of its regressive behavior, where four approach temperatures have been used as fitting parameters. In contrast, TEM showed the highest RMSE values, indicating its lower accuracy compared to the other models considered. In addition, syngas based on the OS approach temperature shows good agreement in prediction after RTM, making it the second most accurate. Furthermore, the kinetic approach shows performance comparable to the OS model. However, it should be noted that the kinetic modeling approach displayed slightly higher RMSE compared to the OS model (the only exception is the CH_4 prediction).

Scatter plot analysis conducted between the experimental values and the predicted values from TEM, RTM, KM, and OS provides valuable information on the predictive precision of these modeling techniques. This analysis focuses specifically on the composition of syngas, particularly H_2, CO, CO_2, and CH_4. In particular, the scatter plots, shown in Fig. 8, reveal that RTM demonstrates the closest proximity of the predicted values to the experimental values, indicating its superior precision in prediction, a finding corroborated by RMSE. In contrast, TEM exhibits tendencies towards overprediction in H_2 and CO, together with underprediction in CO_2 and CH_4, which is consistent with the observations reported by Pilar et al. (2021) [87]. This is probably due to the fact that the estimation of H_2 and CO is compensated by the lack of CO_2 and CH_4. This discrepancy underscores the limitations of TEM, as evidenced by its comparatively poor performance compared to other modeling techniques. On the contrary, the OS values show an intermediate performance, that is, between RTM and TEM. This highlights the utility of OS to provide reasonably accurate predictions while potentially offering computational savings. Although not surpassing RTM's accuracy, OS serves as a viable alternative, paving the way to future studies where biomass gasification models based on a reduced number of parameters can be developed to accurately describe the process. Furthermore, KM demonstrates a similar performance to OS, showing improved predictive accuracy for the prediction of H_2 and CH_4 compared to TEM, although with shortcomings in the prediction of CO

and CO_2. These observations underscore the nuanced nature of modeling techniques and the importance of selecting appropriate methodologies tailored to specific research objectives. It is important to note that these results are highly dependent on the kinetic model and the set of parameters used (collected from the literature). Therefore, more accurate estimations could potentially be obtained if a different kinetic model was applied. Given that TEM exhibits tendencies toward over-prediction in H_2 and CO, simultaneously with underprediction in CO_2 and CH_4, it is clear that residual analysis is necessary to fully understand and anticipate the performance and limitations of this model.

The frequency distribution plots of the residuals of the syngas composition predicted by different models are shown in Fig. 9. It is quite evident that in the case of the RTM the predicted values closely align with the experimental data, as evidenced by the distribution centered around zero residuals, it is also clear that it is over-predicting and under-predicting in certain cases. On the contrary, the TEM demonstrates a tendency for overprediction in H_2 and CO, with residuals predominantly skewed toward the positive x-axis in the frequency distribution graph. Furthermore, for CO_2 and CH_4, the model tends towards under-prediction, indicated by residuals concentrated along the negative x axis. This behavior is consistent with observations from the scatter plots shown in Fig. 8. KM exhibits a pattern of overprediction specifically in the case of CO_2. On the contrary, the OS model presents a more balanced composition prediction compared to TEM and KM, as reflected by the residual distribution. These findings underscore the subtle variations in performance between models, each of which demonstrates distinct characteristics in predicting the composition of syngas. The observed trends in the residual distributions provide valuable information on the efficacy and reliability of each.

4. Conclusions

Woody biomass gasification presents a promising pathway for renewable energy production, but accurately predicting the composition of syngas remains a significant challenge. This study addresses this issue by providing a comprehensive comparative analysis of three modeling approaches TEM, RTM, and KM using flowsheet simulations for woody biomass gasification in a bubbling fluidized bed gasifier. Key findings indicate that RTM achieved the highest accuracy in predicting syngas composition, with an average RMSE of 0.0793, due to its regressive approach that incorporates four fitted temperature parameters. TEM demonstrated the lowest accuracy, with an average RMSE of 0.1735, consistently overpredicting H_2 and CO while underpredicting CO_2 and CH_4. The OS approach (approach temperatures for OS were determined as 0 °C for R2 and -217.233 °C for R3 and R4) showed good precision, with an RMSE of 0.1282, second to RTM and performing comparable to the KM with RMSE of 0.1593, which excelled in the prediction of CH_4. This study sheds some light on the expected discrepancy (compared to the experimental literature data) when some conventional gasification reactor modeling techniques are used. Specifically, the widely used thermodynamic models based on Gibbs minimization are shown to overestimate the H_2 and CO composition (main syngas components). On the other hand, the use of a small set of fitted parameters has been demonstrated to improve composition predictions, as seen in the RTM and OS approaches. These approaches could be practically useful for studies that require fast, simple, and computationally efficient modeling solutions. Future research could focus on extending this framework to various feedstocks, such as woody biomass, plastic waste, and municipal solid waste, as well as exploring co-gasification, incorporating advanced kinetic mechanisms, and developing hybrid models that integrate machine learning with equilibrium and kinetic approaches.

CRediT authorship contribution statement

Usman Khan Jadoon: Writing – review & editing, Writing – original draft, Visualization, Software, Methodology, Investigation, Funding acquisition, Data curation. **Ismael Díaz:** Writing – review & editing, Validation, Supervision, Resources, Project administration, Formal analysis, Conceptualization. **Manuel Rodríguez:** Writing – review & editing, Validation, Supervision, Resources, Project administration, Formal analysis.

Acknowledgements

This project has received funding from the European Union's Horizon 2020 research and innovation programme under the Marie Skłodowska-Curie grant agreement No. 945139.

Appendix A. Supplementary data

Supplementary data to this article can be found online at https://doi.org/10.1016/j.biombioe.2025.107626.

Data availability

The data that has been used in the article is provided in supplementary data.

References

[1] H. Ritchie, P. Rosado, M. Roser, Fossil Fuels, Our World in Data, 2024.
[2] A.I. Osman, L. Chen, M. Yang, G. Msigwa, M. Farghali, S. Fawzy, D.W. Rooney, P.-S. Yap, Cost, environmental impact, and resilience of renewable energy under a changing climate: a review, Environ. Chem. Lett. 21 (2) (2023) 741–764.
[3] I. Malico, R. Nepomuceno Pereira, A.C. Gonçalves, A.M.O. Sousa, Current status and future perspectives for energy production from solid biomass in the European industry, Renew. Sustain. Energy Rev. 112 (2019) 960–977.
[4] Z. Wang, Q. Bui, B. Zhang, T.L.H. Pham, Biomass energy production and its impacts on the ecological footprint: an investigation of the G7 countries, Sci. Total Environ. 743 (2020) 140741.
[5] S.O. Ebhodaghe, E.O. Babatunde, T.O. Ogundijo, A.D. Omotosho, Biomass: challenges and future perspectives, in: S. Thomas, M. Hosur, D. Pasquini, C. Jose Chirayil (Eds.), Handbook of Biomass, Springer Nature Singapore, Singapore, 2023, pp. 1–16.
[6] R.P. Overend, Direct Combustion of Biomass, Renewable Energy Sources Charged with Energy from the Sun and Originated from Earth-Moon Interaction, 2009, pp. 74–100.
[7] D.S. Primadita, I. Kumara, W. Ariastina, A review on biomass for electricity generation in Indonesia, Journal of Electrical, Electron. Inform. 4 (1) (2020) 4.
[8] S. Asif, M. Ahmad, A. Bokhari, C.L. Fatt, M. Zafar, S. Sultana, S. Mir, Chemical conversion in biodiesel refinery, Prospe. Renew. Bioprocess. Future Energy Sys. (2019) 201–217.
[9] Z.I. Rony, M. Mofijur, M. Hasan, S.F. Ahmed, I.A. Badruddin, T.Y. Khan, Conversion of algal biomass into renewable fuel: a mini review of chemical and biochemical processes, Front. Energy Res. 11 (2023) 1124302.
[10] L. Gouveia, P.C. Passarinho, Biomass conversion technologies: biological/biochemical conversion of biomass, Biorefineries: targeting Energy. High Value Products and Waste Valorisation, 2017, pp. 99–111.
[11] P. Basu, Biomass Gasification, Pyrolysis and Torrefaction: Practical Design and Theory, Academic press, 2018.
[12] J. Liu, X. Chen, W. Chen, M. Xia, Y. Chen, H. Chen, K. Zeng, H. Yang, Biomass pyrolysis mechanism for carbon-based high-value products, Proc. Combust. Inst. 39 (3) (2023) 3157–3181.
[13] M. Chaves, C. Torres, C. Tenorio, R. Moya, D. Arias-Aguilar, Syngas characterization and electric performance evaluation of gasification process using forest plantation biomass, Waste Biomass Valoriz. 15 (3) (2024) 1291–1308.
[14] H. Zhang, R. Yoshiie, I. Naruse, Y. Ueki, Degradation of solid oxide fuel cell anodes by the deposition of potassium compounds, Carbon Res. Conver. (2024) 100238.
[15] C. Frilund, S. Tuomi, E. Kurkela, P. Simell, Small-to medium-scale deep syngas purification: biomass-to-liquids multi-contaminant removal demonstration, Biomass Bioenergy 148 (2021) 106031.
[16] N.A.b. Samiran, J. Mohd, apos, M.N.b. afar, C.C. Tung, N. Jo-Han, A review of biomass gasification technology to produce syngas, American-Eurasian, J. Sustain. Agric. (2014) 69+.
[17] U. Arena, Process and technological aspects of municipal solid waste gasification. A review, Waste Manag. 32 (4) (2012) 625–639.
[18] R. Warnecke, Gasification of biomass: comparison of fixed bed and fluidized bed gasifier, Biomass Bioenergy 18 (6) (2000) 489–497.
[19] A. Ramos, E. Monteiro, V. Silva, A. Rouboa, Co-gasification and recent developments on waste-to-energy conversion: a review, Renew. Sustain. Energy Rev. 81 (2018) 380–398.
[20] A. Tremel, D. Becherer, S. Fendt, M. Gaderer, H. Spliethoff, Performance of entrained flow and fluidised bed biomass gasifiers on different scales, Energy Convers. Manag. 69 (2013) 95–106.

[21] A. Chanthakett, M.T. Arif, M.M.K. Khan, A.M.T. Oo, Performance assessment of gasification reactors for sustainable management of municipal solid waste, J. Environ. Manag. 291 (2021) 112661.
[22] U. Arena, F. Di Gregorio, Fluidized bed gasification of industrial solid recovered fuels, Waste Manag. 50 (2016) 86–92.
[23] Z.A.B.Z. Alauddin, P. Lahijani, M. Mohammadi, A.R. Mohamed, Gasification of lignocellulosic biomass in fluidized beds for renewable energy development: a review, Renew. Sustain. Energy Rev. 14 (9) (2010) 2852–2862.
[24] G. Lopez, M. Artetxe, M. Amutio, J. Alvarez, J. Bilbao, M. Olazar, Recent advances in the gasification of waste plastics. A critical overview, Renew. Sustain. Energy Rev. 82 (2018) 576–596.
[25] M. Jeremiáš, M. Pohořelý, K. Svoboda, V. Manovic, E.J. Anthony, S. Skoblia, Z. Beňo, M. Šyc, Gasification of biomass with CO2 and H2O mixtures in a catalytic fluidised bed, Fuel 210 (2017) 605–610.
[26] H.G.M.F. Gomes, M.A.A. Matos, L.A.C. Tarelho, Influence of oxygen/steam addition on the quality of producer gas during direct (air) gasification of residual forest biomass, Energies 16 (5) (2023) 2427.
[27] A. AlNouss, G. McKay, T. Al-Ansari, A comparison of steam and oxygen fed biomass gasification through a techno-economic-environmental study, Energy Convers. Manag. 208 (2020) 112612.
[28] H. Hofbauer, Large scale biomass gasification for electricity and fuels, Energy Organic Mater. (Biomass), Springer (2019) 753–775.
[29] G. Katsaros, D.S. Pandey, A. Horvat, G. Aranda Almansa, L.E. Fryda, J.J. Leahy, S. A. Tassou, Experimental investigation of poultry litter gasification and co-gasification with beech wood in a bubbling fluidised bed reactor – effect of equivalence ratio on process performance and tar evolution, Fuel 262 (2020) 116660.
[30] Y. Tian, D. He, Y. Zeng, L. Hu, J. Du, Z. Luo, W. Ma, Z. Zhang, Experimental research on hydrogen-rich syngas yield by catalytic biomass air-gasification over Ni/olivine as in-situ tar destruction catalyst, J. Energy Inst. 108 (2023) 101263.
[31] B. Vincenti, F. Gallucci, E. Paris, M. Carnevale, A. Palma, M. Salerno, C. Cava, O. Palone, G. Agati, M.V.M. Caputi, D. Borello, Syngas quality in fluidized bed gasification of biomass: comparison between olivine and K-feldspar as bed materials, Sustainability 15 (3) (2023) 2600.
[32] R. Khezri, W.A. Wan Ab Karim Ghani, D.R. Awang Biak, R. Yunus, K. Silas, Experimental evaluation of napier grass gasification in an autothermal bubbling fluidized bed reactor, Energies 12 (8) (2019) 1517.
[33] M. La Villetta, M. Costa, N. Massarotti, Modelling approaches to biomass gasification: a review with emphasis on the stoichiometric method, Renew. Sustain. Energy Rev. 74 (2017) 71–88.
[34] D.S. Pandey, H. Raza, S. Bhattacharyya, Development of explainable AI-based predictive models for bubbling fluidised bed gasification process, Fuel 351 (2023) 128971.
[35] P. Arora, A. Hoadley, S. Mahajani, A. Ganesh, Multi-level modelling of sustainable chemical production: from CFD to LCA, Compu. Aided Chem. Eng. (2016) 499–504. Elsevier.
[36] L. Yan, C.J. Lim, G. Yue, B. He, J.R. Grace, Simulation of biomass-steam gasification in fluidized bed reactors: model setup, comparisons and preliminary predictions, Bioresour. Technol. 221 (2016) 625–635.
[37] Y. Wang, L. Yan, CFD studies on biomass thermochemical conversion, Int. J. Mol. Sci. 9 (6) (2008) 1108–1130.
[38] E. Cima, Evaluation of Comsol Multiphysics for Modelling of Fluidized Bed Combustion, 2015.
[39] A.M.A. Ahmed, A. Salmiaton, T.S.Y. Choong, W.A.K.G. Wan Azlina, Review of kinetic and equilibrium concepts for biomass tar modeling by using Aspen Plus, Renew. Sustain. Energy Rev. 52 (2015) 1623–1644.
[40] A.A. KT, S. P, A. P, Aspen plus simulation of biomass gasification: a comprehensive model incorporating reaction kinetics, hydrodynamics and tar production, Process Inte. Optimizat. Sustain. 7 (1) (2023) 255–268.
[41] S.S. Shahlan, K. Kidam, L. Medic-Pejic, T.A.T. Abdullah, M.W. Ali, Z.Y. Zakaria, Process development of oil palm empty fruit bunch gasification by using fluidised bed reactor for hydrogen gas production, Chem. Eng. Trans. 63 (2018) 559–564.
[42] I. Hannula, E. Kurkela, A semi-empirical model for pressurised air-blown fluidised-bed gasification of biomass, Bioresour. Technol. 101 (12) (2010) 4608–4615.
[43] M.C. Acar, Y.E. Böke, Simulation of biomass gasification in a BFBG using chemical equilibrium model and restricted chemical equilibrium method, Biomass Bioenergy 125 (2019) 131–138.
[44] M. Ajorloo, M. Ghodrat, J. Scott, V. Strezov, Recent advances in thermodynamic analysis of biomass gasification: a review on numerical modelling and simulation, J. Energy Inst. 102 (2022) 395–419.
[45] D.T. Pio, L.A.C. Tarelho, Empirical and chemical equilibrium modelling for prediction of biomass gasification products in bubbling fluidized beds, Energy 202 (2020) 117654.
[46] R. Radmanesh, J. Chaouki, C. Guy, Biomass gasification in a bubbling fluidized bed reactor: experiments and modeling, AIChE J. 52 (12) (2006) 4258–4272.
[47] M. Dhrioua, K. Ghachem, W. Hassen, A. Ghazy, L. Kolsi, M.N. Borjini, Simulation of biomass air gasification in a bubbling fluidized bed using aspen plus: a comprehensive model including tar production, ACS Omega 7 (37) (2022) 33518–33529.
[48] A. Velázquez-Hernández, J.E. Aguillón-Martínez, Aspen plus simulation of sargassum for quality synthesis gas, Heliyon 9 (7) (2023) e17731.
[49] M. Puig-Gamero, D.T. Pio, L.A.C. Tarelho, P. Sánchez, L. Sanchez-Silva, Simulation of biomass gasification in bubbling fluidized bed reactor using aspen plus, Energy Convers. Manag. 235 (2021) 113981.
[50] A. Gómez-Barea, R. Arjona, P. Ollero, Pilot-Plant gasification of olive stone: a technical assessment, Energy Fuel. 19 (2) (2005) 598–605.
[51] U. Arena, F. Di Gregorio, M. Santonastasi, A techno-economic comparison between two design configurations for a small scale, biomass-to-energy gasification based system, Chem. Eng. J. 162 (2) (2010) 580–590.
[52] S. Kaewluan, S. Pipatmanomai, Gasification of high moisture rubber woodchip with rubber waste in a bubbling fluidized bed, Fuel Process. Technol. 92 (3) (2011) 671–677.
[53] P. Lahijani, Z.A. Zainal, Gasification of palm empty fruit bunch in a bubbling fluidized bed: a performance and agglomeration study, Bioresour. Technol. 102 (2) (2011) 2068–2076.
[54] M. Kwapinska, G. Xue, A. Horvat, L.P.L.M. Rabou, S. Dooley, W. Kwapinski, J. J. Leahy, Fluidized bed gasification of torrefied and raw grassy biomass (miscanthus × gigantenus). The effect of operating conditions on process performance, Energy Fuel. 29 (11) (2015) 7290–7300.
[55] D. Serrano, S. Sánchez-Delgado, C. Sobrino, C. Marugán-Cruz, Defluidization and agglomeration of a fluidized bed reactor during Cynara cardunculus L. gasification using sepiolite as a bed material, Fuel Process. Technol. 131 (2015) 338–347.
[56] T. Robinson, B. Bronson, P. Gogolek, P. Mehrani, Comparison of the air-blown bubbling fluidized bed gasification of wood and wood–PET pellets, Fuel 178 (2016) 263–271.
[57] S. Nilsson, A. Gómez-Barea, D. Fuentes-Cano, P. Haro, G. Pinna-Hernández, Gasification of olive tree pruning in fluidized bed: experiments in a laboratory-scale plant and scale-up to industrial operation, Energy Fuel. 31 (1) (2017) 542–554.
[58] D.T. Pio, L.A.C. Tarelho, M.A.A. Matos, Characteristics of the gas produced during biomass direct gasification in an autothermal pilot-scale bubbling fluidized bed reactor, Energy 120 (2017) 915–928.
[59] J. George, P. Arun, C. Muraleedharan, Assessment of producer gas composition in air gasification of biomass using artificial neural network model, Int. J. Hydrogen Energy 43 (20) (2018) 9558–9568.
[60] R. Khezri, W.A.A.K. Ghani, D.R.A. Biak, R. Yunus, K. Silas, Experimental evaluation of napier grass gasification in an autothermal bubbling fluidized bed reactor, Energies 12 (8) (2019).
[61] W. Lan, G. Chen, X. Zhu, X. Wang, X. Wang, B. Xu, Research on the characteristics of biomass gasification in a fluidized bed, J. Energy Inst. 92 (3) (2019) 613–620.
[62] I. Ul Hai, F. Sher, A. Yaqoob, H. Liu, Assessment of biomass energy potential for SRC willow woodchips in a pilot scale bubbling fluidized bed gasifier, Fuel 258 (2019) 116143.
[63] R. Timsina, R.K. Thapa, B.M.E. Moldestad, M.S. Eikeland, Experiments and computational particle fluid dynamics simulations of biomass gasification in an air-blown fluidized bed gasifier, Int. J. Energy Produc. Manage. 5 (2) (2020) 102–114.
[64] X. Wang, Z. Zhong, B. Jin, Experimental evaluation of biomass medium-temperature gasification with rice straw as the fuel in a bubbling fluidized bed Gasifier, Int. J. Chem. React. Eng. 18 (1) (2020) 20190147.
[65] J.C. Bandara, R. Jaiswal, H.K. Nielsen, B.M.E. Moldestad, M.S. Eikeland, Air gasification of wood chips, wood pellets and grass pellets in a bubbling fluidized bed reactor, Energy 233 (2021) 121149.
[66] Y. Tian, D. He, Y. Zeng, L. Hu, J. Du, Z. Luo, W. Ma, Z. Zhang, Experimental research on hydrogen-rich syngas yield by catalytic biomass air-gasification over Ni/olivine as in-situ tar destruction catalyst, J. Energy Inst. 108 (2023).
[67] N. Mukahar, Performance comparison of k nearest neighbor classifier with different distance functions, AIP Conf. Proc. (2024). AIP Publishing.
[68] L.P.R. Pala, Q. Wang, G. Kolb, V. Hessel, Steam gasification of biomass with subsequent syngas adjustment using shift reaction for syngas production: an Aspen Plus model, Renew. Energy 101 (2017) 484–492.
[69] M. Puig-Arnavat, J.C. Bruno, A. Coronas, Review and analysis of biomass gasification models, Renew. Sustain. Energy Rev. 14 (9) (2010) 2841–2851.
[70] D.A. Rodriguez-Alejandro, H. Nam, A.L. Maglinao Jr., S.C. Capareda, A.F. Aguilera-Alvarado, Development of a modified equilibrium model for biomass pilot-scale fluidized bed gasifier performance predictions, Energy 115 (2016) 1092–1108.
[71] A.M.L. Násner, E.E.S. Lora, J.C.E. Palacio, M.H. Rocha, J.C. Restrepo, O. J. Venturini, A. Ratner, Refuse Derived Fuel (RDF) production and gasification in a pilot plant integrated with an Otto cycle ICE through Aspen plus™ modelling: thermodynamic and economic viability, Waste Manag. 69 (2017) 187–201.
[72] H. Gu, Y. Tang, J. Yao, F. Chen, Study on biomass gasification under various operating conditions, J. Energy Inst. 92 (5) (2019) 1329–1336.
[73] A. Abdelrahim, P. Brachi, G. Ruoppolo, S.D. Fraia, L. Vanoli, Experimental and numerical investigation of biosolid gasification: equilibrium-based modeling with emphasis on the effects of different pretreatment methods, Ind. Eng. Chem. Res. 59 (1) (2019) 299–307.
[74] D. Neves, H. Thunman, A. Matos, L. Tarelho, A. Gómez-Barea, Characterization and prediction of biomass pyrolysis products, Prog. Energy Combust. Sci. 37 (5) (2011) 611–630.
[75] W.M. Champion, C.D. Cooper, K.R. Mackie, P. Cairney, Development of a chemical kinetic model for a biosolids fluidized-bed gasifier and the effects of operating parameters on syngas quality, J. Air Waste Manag. Assoc. 64 (2) (2014) 160–174.
[76] G. Groppi, E. Tronconi, P. Forzatti, M. Berg, Mathematical modelling of catalytic combustors fuelled by gasified biomasses, Catal. Today 59 (1–2) (2000) 151–162.
[77] L.D. Smoot, P.J. Smith, Coal Gasification and Combustion, Plenum Press, New York, 1985.
[78] C.K. Westbrook, F.L. Dryer, Chemical kinetic modeling of hydrocarbon combustion, Prog. Energy Combust. Sci. 10 (1) (1984) 1–57.
[79] A.M. Gonzalez, E.E.S. Lora, J.C.E. Palacio, O.A.A. del Olmo, Hydrogen production from oil sludge gasification/biomass mixtures and potential use in hydrotreatment processes, Int. J. Hydrogen Energy 43 (16) (2018) 7808–7822.
[80] A. Gómez-Barea, B. Leckner, Modeling of biomass gasification in fluidized bed, Prog. Energy Combust. Sci. 36 (4) (2010) 444–509.

[81] P. Morf, P. Hasler, T. Nussbaumer, Mechanisms and kinetics of homogeneous secondary reactions of tar from continuous pyrolysis of wood chips, Fuel 81 (7) (2002) 843–853.
[82] S. Chianese, J. Loipersböck, M. Malits, R. Rauch, H. Hofbauer, A. Molino, D. Musmarra, Hydrogen from the high temperature water gas shift reaction with an industrial Fe/Cr catalyst using biomass gasification tar rich synthesis gas, Fuel Process. Technol. 132 (2015) 39–48.
[83] A. Lampropoulos, I.G. Zubillaga, R. Pérez-Vega, N. Ntavos, Y. Fallas, G. Varvoutis, Preliminary experimental results and modelling study of olive kernel gasification in a 2 MWth BFB gasifier, Processes 10 (10) (2022) 2020.
[84] Y. Gao, M. Wang, A. Raheem, F. Wang, J. Wei, D. Xu, X. Song, W. Bao, A. Huang, S. Zhang, Syngas production from biomass gasification: influences of feedstock properties, reactor type, and reaction parameters, ACS Omega 8 (35) (2023) 31620–31631.
[85] N. Gao, A. Li, C. Quan, Y. Qu, L. Mao, Characteristics of hydrogen-rich gas production of biomass gasification with porous ceramic reforming, Int. J. Hydrogen Energy 37 (12) (2012) 9610–9618.
[86] F.M. Alptekin, M.S. Celiktas, Review on catalytic biomass gasification for hydrogen production as a sustainable energy form and social, technological, economic, environmental, and political analysis of catalysts, ACS Omega 7 (29) (2022) 24918–24941.
[87] M. Pilar González-Vázquez, F. Rubiera, C. Pevida, D.T. Pio, L.A. Tarelho, Thermodynamic analysis of biomass gasification using aspen plus: comparison of stoichiometric and non-stoichiometric models, Energies 14 (1) (2021) 189.